ADVANCES IN ROBOTIC IN-ORBIT ASSEMBLY OF LARGE-APERTURE SPACE TELESCOPES

Virtual Conference 19–23 October 2020

Manu H. Nair[1*], Chakravarthini M. Saaj[1], Sam Adlen[2], Amir G. Esfahani[1], Steve Eckersley[3]

[1]Lincoln Centre for Autonomous Systems, University of Lincoln, United Kingdom, LN6 7TS
*Corresponding Author: 18710796@students.lincoln.ac.uk, (MSaaj, AGhalamzanEsfahani)@lincoln.ac.uk
[2]Satellite Applications Catapult Ltd, Harwell, Didcot, United Kingdom, OX11 0QR, Sam.Adlen@sa.catapult.org.uk
[3]Surrey Satellite Technology Limited, Guildford, United Kingdom, GU2 7YE, S.Eckersley@sstl.co.uk

ABSTRACT

Modular Large Aperture Space Telescopes (LAST) hold the key to future astronomical missions in search of the origin of the cosmos. Robotics and Autonomous Systems technology would be required to meet the challenges associated with the assembly of such high value infrastructure in orbit. In this paper, an End-Over-End walking robot is selected to assemble a 25m LAST. The dynamical model, control architecture and gait pattern of the E-Walker are discussed. The key mission requirements are stated along with the strategies for scheduling the assembly process. A mission concept of operations (ConOps) is proposed for assembling the 25m LAST. Simulation results show the precise trajectory tracking of the E-Walker for the chosen mission scenario.

Keywords: In-Orbit Assembly; Large-Aperture Space Telescope; End-Over-End Walking Robot; Precise Manipulation; Gait Pattern; Mission ConOps

1 INTRODUCTION

Space has found itself amidst numerous missions benefiting mankind's urge to explore the solar system and beyond. With Robotics, Automation and Autonomous Systems (RAAS) helping the space community achieve success in various planetary missions, there is a move to launch various in-orbit missions in the upcoming decade, tackling the extremities of the space environment, for performing tasks like in-space manufacturing, assembly, maintenance, repairs of spacecraft and active debris removal [1]. Telescopes have helped astronomers visualize distant stars, asteroids and galaxies in their search for the origin of life. However, the Earth-based Space observatories have to overcome some perpetual troublemakers like atmospheric disturbances, air turbulence and light pollution, resulting in an image with significant loss of resolution. Addressing these issues gave way to the idea of placing telescopes in Space [2].

Figure 1. SpaceX Dragon and Canadarm2 [1]

Although the functional Hubble Space Telescope (HST) and the new James Webb Space Telescope (JWST), expected to be launched by 2021, are exceptional examples, Large-Aperture Space Telescopes (LASTs) are necessary for a higher spatial resolution. With the current limitations in the fairing capacity of the launch vehicles, LAST cannot be manufactured monolithically [3]. It is highly likely that RAAS could facilitate assembly of modular LAST in-space [4, 5]. The recently published UK research and development roadmap highlights the importance and potential the UK sees in in-space robotic missions [6]

In this paper, a 25m LAST is considered for in-space assembly [7]. An extensive review of possible robotic solutions presented in [8] and the proposed architecture in [4, 5, 7, 9], lead to the choice of a 5 degrees-of-freedom (DoF) End-Over-End Walking Robot (E-Walker) to undertake the assembly of this 25m LAST. The E-Walker is inspired by the Canadarm2, already onboard the International Space Station (ISS) and the European Robotic Arm (ERA). This paper presents an overview of a dynamic model of the five DoF E-Walker along with its functionality. Simulation results of the E-Walker's precise motion control over a few cycles are also presented along with the E-Walker following a trajectory corresponding to a real mission scenario. To provide a deeper insight into the assembly operation, a potential mission concept is discussed with its workflow represented using an algorithm. Overall, this paper illustrates the feasibility of assembling the 25m LAST, using E-Walkers in a cost and time-efficient manner.

2 MISSION REQUIREMENTS

This paper addresses a robotic in-orbit assembly of a 25m LAST. A few key requirements for the successful completion of the mission are:

1) The robotic manipulator should be mobile around the Base Spacecraft (B_{sc}) and be able to walk across the truss. The assembly of the truss is not directly addressed in this paper.

2) The mobile manipulator should have sufficient reachability to assemble the farthest mirror module.

3) B_{sc} and Truss to incorporate connector ports to help the robotic manipulator to be mobile around them.

4) During the assembly process, the mobile manipulator should keep a safe distance of 0.5-1m with the already assembled fragile mirrors, to prevent collision.

5) The integrated system, comprising of the Base Spacecraft and the mobile manipulator shall consume minimum on-board power, have low lifting-mass cost and risk of debris generation, with minimum control complexity during the assembly process.

3 E-WALKER DESIGN, DYNAMIC MODEL, CONTROL AND GAIT PATTERN ANALYSIS

3.1 E-Walker Design

The concept of a mobile walking manipulator evolved following the successful deployment of the Canadarm2 arm for servicing and maintenance onboard the ISS. The 5 DoF E-Walker presented in this paper is a derivative of Canadarm2 and it meets the essential mission requirements identified in Section 2 (Fig. 2). Unlike any other fixed-to-base robotic manipulator, the E-Walker has the capability to be mobile around its base platform in any direction [8]. The movement can be considered as a replica of the "Queen" in the game of Chess, in a 3D space. During each step of the motion, one joint of the E-Walker, Joint-1 (J_1) or Joint-5 (J_5) here, is locked to the B_{sc}. Understandably, in each phase of motion, the E-Walker acts as a fixed-to-base robot manipulator.

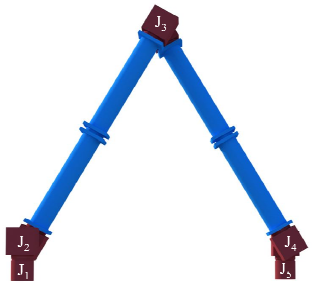

Figure 2. E-Walker Architecture

3.3 Gait pattern analysis

Figure 4 explains the motion of the E-Walker. The E-Walker starts at an initial position as shown in Fig. 4a. During Phase-1, J_1 is fixed to the base and J_5's motion is tracked (Fig. 4b). Figure 4c shows Phase-2, where J_5 is locked and J_1's motion is tracked, completing the first cycle of motion. The cyclic motion helps the E-Walker to move forwards or backwards in any direction. To facilitate the E-Walker's motion in a real mission scenario, B_{sc} and Truss would have connector points for the E-Walker. The workspace of the E-Walker is therefore only limited based on the availability of the connector points. This feature helps in the design process as a dimensionally large robot architecture can be avoided, addressing the 5th mission requirement under Section 2.

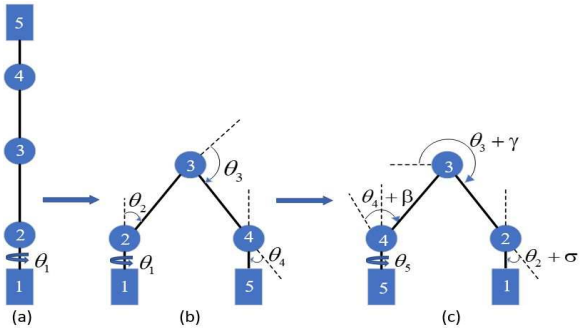

Figure 4. Cycle-1 Walking Pattern of an E-Walker: (a) Initial Position (b) Phase-1 and (c) Phase-2

3.2 Dynamic Model and Control Architecture

The dynamic equation of torque for the 5 joints is computed using the Euler-Lagrange method as $\boldsymbol{\tau} = \mathbf{D}(\theta)\ddot{\boldsymbol{\theta}} + \mathbf{C}(\theta,\dot{\theta})\dot{\boldsymbol{\theta}} + \mathbf{G}(\theta)$, where $\mathbf{D}(\theta) \in \mathbb{R}^{5\times5}$ is the inertia matrix. The $\mathbf{C}(\theta,\dot{\theta}) \in \mathbb{R}^{5\times5}$ comprises of the Coriolis and centrifugal terms. During a space operation, potential energy is neglected. Although, for the Earth-based analog testing, potential energy is taken into consideration. The matrix $\mathbf{G}(\theta) \in \mathbb{R}^{5\times1}$ is the Gravity matrix which represents the potential energy terms [10].

The Computed Torque Control (CTC) has an inner forward loop and a feedback outer loop. In the inner loop, a desired trajectory is selected and a tracking error term is defined. In the feedback outer loop, the control input is selected based on the controller used, to stabilize the error over time.

A Proportional-Integral-Derivative (PID) controller is used with CTC, governed by the control law: $\boldsymbol{\tau} = \mathbf{D}(\theta)\boldsymbol{\tau}' + \mathbf{C}(\theta,\dot{\theta})\dot{\boldsymbol{\theta}} + \mathbf{G}(\theta)$, where control input, $\boldsymbol{\tau}' = \ddot{\boldsymbol{\theta}}^{d} + \boldsymbol{K}_p(\boldsymbol{\theta}^{d} - \boldsymbol{\theta}) + \boldsymbol{K}_i\int(\boldsymbol{\theta}^{d} - \boldsymbol{\theta})\mathrm{dt} + \boldsymbol{K}_d(\dot{\boldsymbol{\theta}}^{d} - \dot{\boldsymbol{\theta}})$.

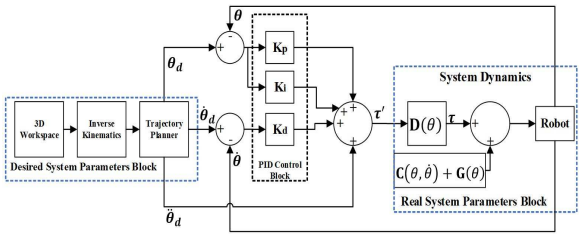

Figure 3. E-Walker Control Architecture

The PID controller used in the system block tracks the desired joint angles in both the phases, without exceeding the joint torque limits, ensuring precise motion along the desired trajectory. In the closed-loop control architecture shown in Fig. 3, $\boldsymbol{\theta}_d$, $\dot{\boldsymbol{\theta}}_d$ and $\ddot{\boldsymbol{\theta}}_d$ are the vectors of the desired joint angles, velocities and accelerations. $\boldsymbol{\theta}$ and $\dot{\boldsymbol{\theta}}$ are the vectors of the real joint angles and velocities. $\boldsymbol{K}_p$, $\boldsymbol{K}_i$ and $\boldsymbol{K}_d$ are the proportional, integral and differential gains of the PID Controller [10].

4 FEATURES OF LAST, TRUSS AND B_{sc}

4.1 LAST

Placing a LAST in space would enable numerous scientific discoveries with its capability to visualise farther and fainter objects. However, constructing such a huge telescope is extremely challenging. The key issues associated with the current state-of-the-art technology to place a LAST in space is that the Primary Mirror (PM) cannot be monolithically manufactured and a folded-wing design cannot be implemented as seen in JWST. Even if a gigantic monolithic mirror is manufactured, maintenance and stowing it into the launch vehicles like Ariane 64, with a maximum inner diameter of 4.57m and the currently under development New Glenn is not feasible [7].

To meet these challenges, a segmented design approach is to be used [11]. The 25m PM, presented in this paper is divided equally to be build using 18 Primary Mirror Segments (PMS). Each PMS is build using 19 hexagonally-shaped Primary Mirror Units (PMUs) having a maximum dimension of 1m. Fig. 6 shows the assembled 25m LAST.

Each PMU would be placed on a hexagonal backplane, with each side incorporated with a connector point as shown in Fig. 5, for the E-Walker to perform pick-and-place operations. The PMUs would be stacked in the storage spacecraft. The storage spacecraft would then be lifted off to be docked onto the base spacecraft, serving as the collection point for the E-Walker in the assembly line.

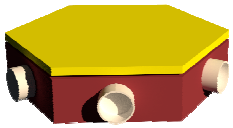

Figure 5. PMU with backplane

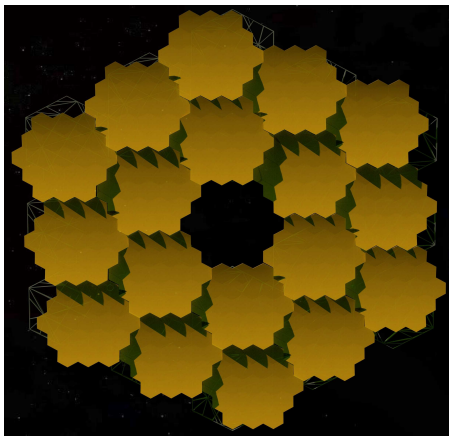

Figure 6. Artistic impression of an assembled 25m LAST

4.2 Truss

As discussed in Section 4.1, the 18 PMSs are to be placed on the truss [7]. Figure 7 shows the approximate mirror positions on the truss. 6 PMSs would be placed in the inner-ring, numbered (blue squares 1-6) and 12 PMSs in the outer-ring, numbered 7-18 in green squares. The yellow circles are the connector points on the truss. The connector points would facilitate the E-Walker's motion to place the PMS. During the assembly, some of the connector points would be used for the E-Walker to traverse around to organise the PMS. Rest of the connector points could be used as safe positions when required.

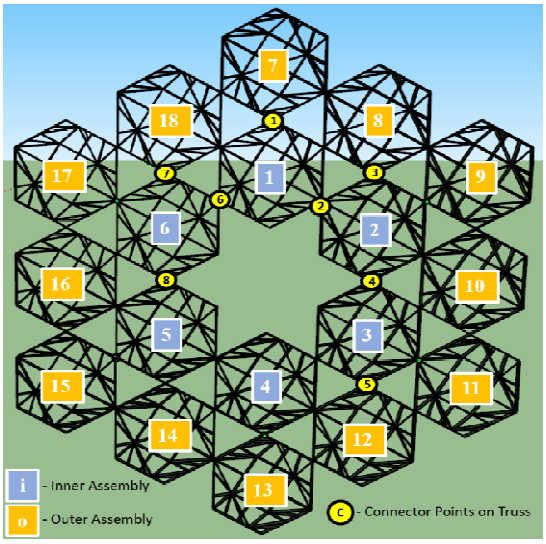

Figure 7. Truss – Mirror positions, Connector points

4.3 Base Spacecraft

The Base Spacecraft will have connector points incorporated in their design to help the E-Walker traverse to the truss and back. The connector points are placed in symmetric order. The B_{sc} in the current in this paper has 25 connector points named (Bsc_C_1-$B_{sc}\_C_{25}$). Fig. 8 shows one half of the B_{sc}.

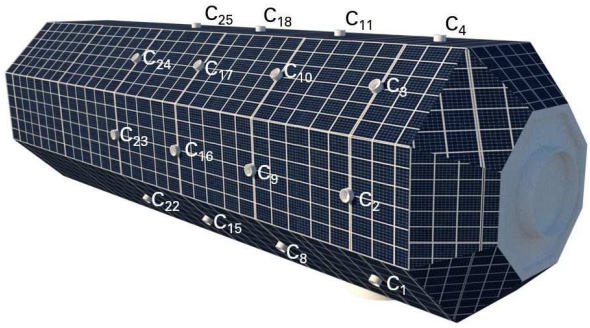

Figure 8. Side view of the Base Spacecraft

5 ASSEMBLY STRATEGY

The assembly of a 25m LAST is a mission which involves the E-Walker performing multiple pick and place operations by moving around the B_{sc} and truss. The idea is to systematically manage the operations between the spacecraft, mobile manipulator and the truss. The mirrors have to be carefully handled and clearance has to be kept all the time to avoid any generation of debris resulting from a collision. The main challenge is to provide a quick and efficient plan to execute the complete task. Addressing the challenge:

1) The strategy required is to assemble the outer ring mirrors first to allow the E-Walker to walk around the truss during the assembly process. The inner ring can be assembled with the robot placed on the B_{sc}.

2) To fill in the outer ring mirror positions, the PMUs can be initially assembled in any of the inner ring positions. The assembled PMS can then be placed onto the outer ring position, with the E-Walker moving to the relevant connector point on the truss.

3) When a situation arises, where the E-Walker has to perform pick-and-place operations on a connector point on the truss, then it has to make sure that it is not placing a PMU/PMS in the nearest/ 'in-zone' mirror locations as it would lead to a collision. For e.g., if the E-Walker is on connector point 5 (C_5) on the truss, it should make sure that it is not assembling/ placing the mirrors in mirror position 3 or 12. Here, 3 and 12 are the in-zone mirror locations for C_5.

6 MISSION ConOps

The proposed mission concept involves two E-Walkers, namely EW_1 and EW_2 working collaboratively to assemble the 25m LAST. The choice of the number of E-Walkers was made based upon the time required for the completion of the assembly, cost of mission, power requirements, lifting-mass, control and planning complexity. Contrary to the current state of interest in the use of a single robot manipulator, two E-Walkers are used as it maintains a balance for a quicker assembly with minimal increase in the other factors. This mission concept lays a foundation for future missions where the collective modular assembly would be required for a 50/100m LAST [6]. More number of E-Walkers would be needed then. There are mainly 2 modes of operation. Mode 1 involves EW_1 and EW_2 working together. In Mode 2, EW_1 and EW_2 take up individual responsibilities to work as a parallel assembly line.

List of Variables

a= In use Connector number array on B_{sc}

b= In use Connector number array on Truss

p'= Array of Initial Mirror position locations on Truss

p= Array of Final Mirror Positions arranged in the the required sequence of placement

p= Array of final mirror positions arranged in the the sequence of placement (positions of 12 PMS)

p_{2l}= Array of final mirror positions to be assembled by EW_1 on left-half of the truss

p_{2r}= Array of final mirror positions to be assembled by EW_2 on right-half of the truss (Positions in sequence: 8, 4, 3, 2)

mode = select the mode of operation.

mode 1: where EW1 and EW2 work together.

mode 2: EW1 and EW2 work parallelly on the left half and right half mirrors. p_{2l} and p_{2r} mirror arrays would be assembled in mode 2.

c= PMS counter.; d= Array of E-Walker Numberings

m= array index of a

n= array index of b

i'= array index of p'

i= array index of p

i_1= array index of p_{2l}

i_2= array index of p_{2r}

k= array index of c

l= array index of d

Ⓐ - assembles/assembling

PMS – Primary Mirror Segment

EW- End-Over-End Walker

Pos - Position
B_{sc}_C – Base Spacecraft Connector

6.1 Initialisation
Initialise the required parameters.

```
1 a = [8,14], b = [5,4,8,6,2], p' = [4,5,3],
2 p = [13,11,10,12,9,14,15,16,17,18], p2l = [7,5,6,1],
3 p2r = [8,4,3,2], c = [3,5,10,12,18], d = [2,1]
4 m = n = i = i' = k = l = mode = i1 = i2 = 1
```

6.2 State Check
Check whether E-Walkers are in the desired connector points on the Base Spacecraft and if the mirror assembly is incomplete.

```
5 while (EWd(l) @ Bsc_Ca(m+1) && EWd(l+1) @
          Bsc_Ca(m) && i<=18)
```

6.3 Mode:1
Both E-Walkers work together to fill in 10 of the 12 outer ring mirror positions (variable p).

```
6      if mode = 1
7        EW1+EW2 Ⓐ PMS in Pos p'(i')
8        Move EWd(l) to Cb(n)
9        EWd(l) places PMS from Pos p'(i') ->Pos p(i)
10        if i=c(k)
11          if i>=5
12            if i>=10
13            then mode=2; n=n+1; k=k+1; i'=i'+1;
14            else
15            EWd(l+1) Ⓐ new PMS in Pos p'(i')
16            EWd(l) moves back to Bsc_Ca(m+1)
17            d([1 2]) = d([2 1]);
18            a([1 2]) = a([2 1]);
19            n = n+1; i = i+1; k = k+1;
20            end
21          else
22            EWd(l+1) starts Ⓐ new PMS in Pos p'(i')
23            n = n+1; i = i+1; k = k+1;
24            EWd(l) moves back to Bsc_Ca(m+1)
25          end
26        else
27          EWd(l+1) starts Ⓐ  new PMS in Pos p'(i')
28          i = i+1;
29          EWd(l) moves back to Bsc_Ca(m+1)
30        end
31    end
```

6.4 Mode: 2
Post Mode-1, the assembly of 8 PMSs, i.e. Pos. 1, 2, 3, 4, 5, 6, 7 and 8 remains. EW_1 and EW_2 work independently of each other to fill out the rest of the mirror positions. EW_1 is assigned the responsibility of assembly in the left half of the truss, whereas EW_2 takes care of the right half. This strategy helps with quicker assembly with limited movements.

```
32   if mode = 2
33     if i>=c(k)
34       if i>=12
35         if i==18
36           then 'Assembly is Over';
37         end
38       else
39         i1 = i1+1; i2 = i2+1;
40         EWd(l) Ⓐ MS in Pos p2l(i1)
41         EWd(l+1) Ⓐ MS in Pos p2r(i2)
42         i = i+2;
43       end
44     else
45       EWd(l) Ⓐ PMS in Pos p'(i')
46       EWd(l+1) Ⓐ PMS in Pos p'(i'+1)
47       Move EWd(l) to Cb(n)
48       Move EWd(l+1) to Cb(n+1)
49       EWd(l) places PMS in Pos p2l(i1)
50       i =i +1;
51       EWd(l+1) places PMS in Pos p2r(i2)
52       i = i+1;
53       EWd(l) moves back to Bsc_Ca(m+1)
54       EWd(l+1) moves back to Bsc_Ca(m)
55     end
56   end
57 end
```

6.4 Mission Flow

The algorithm presented above involves a sequence of operations summarized below:

1) Initially, the position of EW_1 and EW_2 is checked on the B_{sc}
2) The assembly can be started from either half of the truss. In this mission flow, the right-half outer-ring positions are filled first.
3) During the assembly, it is assumed that the PMUs are readily available for the E-Walkers to pick and place.
4) The mode is set to 1 during the beginning of the assembly.
5) The process begins with EW_1 and EW_2 assembling the first PMS in the inner-ring Pos 4.
6) Post assembly, EW_2 walks on to C_5 on the truss to pick the PMS from Pos. 4 and place it in Pos. 13.
7) EW_1 then continues to assemble the next PMS in the inner ring position, while EW_2 returns to B_{sc}_C_{14} to assist EW_1.

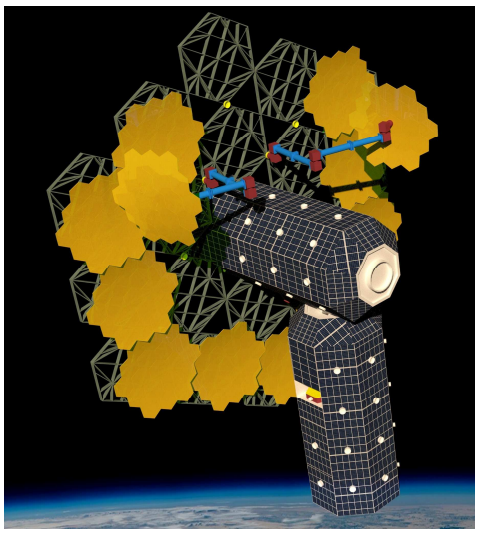

Figure 9. Mode 2 – EW_1 at C_6 placing a PMS in Pos. 7; EW_2 at C_2 placing a PMS in Pos. 8

8) Pos. 11 and Pos. 10 are filled in a similar manner.
9) Pos. 12 and Pos. 9 are filled in a similar manner with EW_2 walking onto C_4 for the pick-and-place operation.
10) Hereafter, there is a switch. As most of the right half outer-ring assembly is over, the left-half assembly is taken care of by EW_1.
11) EW_1 and EW_2 assemble the next PMS. Once assembled, EW_1 moves onto C_8 on the truss to place the PMS in Pos. 14. EW_1 moves back to B_{sc}_C_8 to assist EW_2 in the assembly of the PMS in Pos. 4.
12) Step 11 is repeated to fill in Pos. 15, 16, 17 and 18.
13) 10 PMSs are placed. 2 outer-ring and 6 inner-ring positions remain to be assembled.
14) Now, the mode is switched to 2.
15) In mode 2, EW_1 and EW_2 have individual responsibilities of assembling the PMS and perform the pick-and-place operation in their halves.
16) EW_1 assembles a PMS in inner-ring Pos. 5, and EW_2 in Pos. 3. EW_1 moves onto C_6 and EW_2 to C_2. EW_1 places the PMS in Pos. 7, while EW_2 in Pos. 8 as seen in Fig. 9
17) EW_1 assembles the inner ring Pos. 5, 6 and 1, while EW_2 completes the assembly by filling up Pos. 4, 3 and 2.

7 SIMULATION RESULTS

For a clear understanding of the motion of the E-Walker, only EW_1's motion is considered in the simulation results. EW_1 and EW_2 would have similar performances while traversing in a straight line. For a practical mission scenario, EW_2's cyclic motion would vary only with respect to the connector points via which its traversing. Simulation results showcase the EW_1 capability to track the desired trajectory within the joint torque limits. To avoid any sudden discontinuity in acceleration, a 5th order polynomial function given by *P(T')* that satisfies all initial and final conditions for the joint parameters is used to define the trajectory of the E-Walker [12, 13].
The initial and final conditions are as follows:

1) $\theta_i(0) = \theta_{i_0}$ and $\theta_i(t_f) = \theta_{i_f}$
2) $\dot{\theta}_i(0) = 0$ and $\dot{\theta}_i(t_f) = 0$
3) $\ddot{\theta}_i(0) = 0$ and $\ddot{\theta}_i(t_f) = 0$

$$\theta_i^d = \theta_{i_0} + (\theta_{i_f} - \theta_{i_0})P(T').$$

A straight-line trajectory over a few cycles and a trajectory corresponding to a realistic mission scenario is presented.

7.1 Straight-line trajectory over 3 cycles

For the simulation results for a straight-line motion, the EW_1's link length is considered to be 0.3 m. The offset distance is 0.1m. This gives the insight that in each phase, the E-Walker should walk a distance of 0.3m, which is the distance between the two joints.

7.1.1 Joint Angle

In the simulation shown, only 1 cycle of EW_1's motion is taken into consideration for clarity. Cycles 2 and 3 were found to follow the same configuration over time. Joint configuration A = [0;0;0;0;0], B = [0;30;120;30;0], C = [0; -30; -120; -30; 0]. Phase-1 (A-B) is run from t = 0:10 and Phase-2 (C-B) is run from t = 10:30. Post completion of Phase-1, the joint configuration attained by the E-Walker (here, B) is made equal to the required starting configuration for Phase-2 (C). For 3 cycles, the simulation time would be 100 seconds. For the 2nd and 3rd cycle, Phase-1

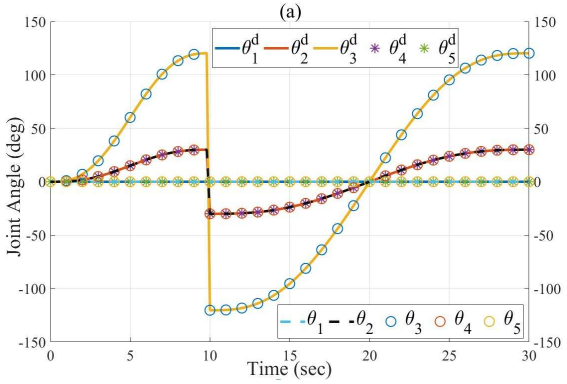

Figure 10. EW_1 - Cycle 1: Joint angles

would begin from configuration C and go to configuration B, requiring 20 seconds to execute. Fig. 10 shows that the desired and real joint angle configurations match at every time step.

7.1.2 Joint Velocity

From Fig. 11, it is seen that the joint velocities follow the initial (0 deg/sec) and final (0 deg/sec) desired values in each phase. The peak velocity of each joint is achieved halfway through the phase.

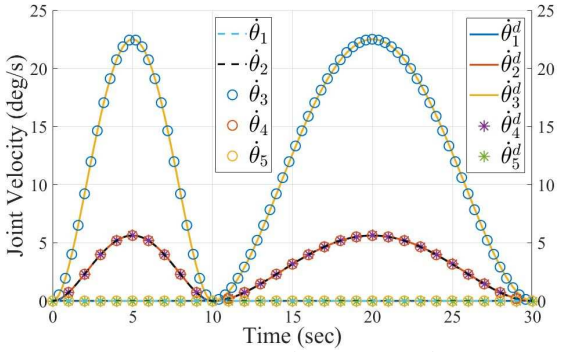

Figure 11. EW₁ - Cycle 1: Joint velocities

7.1.3 Joint Torque

Figure 12 shows that in Phase-1, J_2 experiences the maximum negative torque as the E-Walker moves in the direction of gravity. In Phase-2, J_4 experiences the maximum positive torque in the first lifting half and a negative torque in the second falling half, showcasing the desired performance. The maximum absolute torque experienced under gravity is ~2.3Nm. Without gravity, the maximum absolute torque experienced is ~0.011Nm. The pattern is seen to follow for the consecutive cycles.

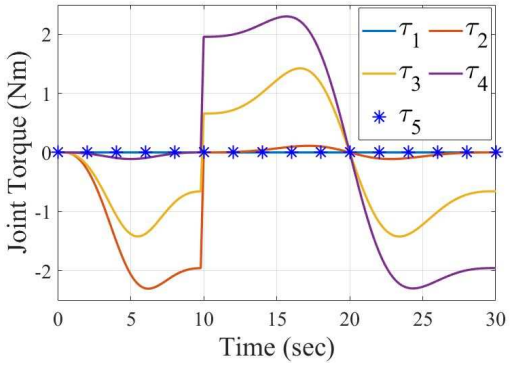

Figure 12. EW₁ - Cycle 1: Joint torques

7.1.3 Trajectory Plot

The trajectory plot in Fig. 13 shows the E-Walker's motion over 3 cycles in a straight-line trajectory. In Cycle 1, with J_1 fixed to the base and J_5's motion being tracked in Phase-1, the E-Walker traverses a distance of 0.3m. In Phase-2, J_1's motion is tracked with J_5 locked. The E-Walker walks a distance of

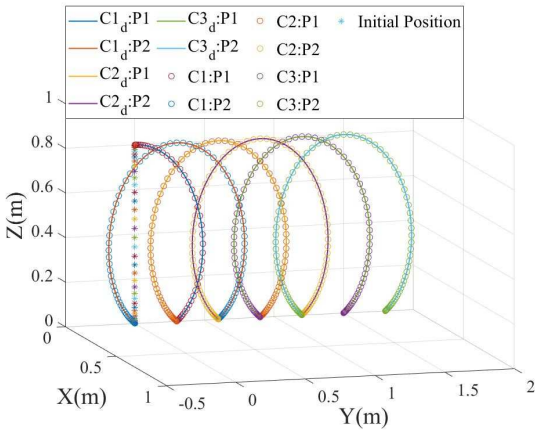

Figure 13. EW₁ - Cycle 1-3: Trajectory

0.6m. Simulation results show that the E-Walker traversed a distance of 1.8m in 3 cycles, which matches the desired result.

7.2 Trajectory Tracking for a Practical Mission Scenario

The trajectory during a real mission scenario is presented in Fig. 14, where trajectory 1 shows the E-Walker starting from an initial position at connector point $B_{sc}\_C_{11}$ and traversing to $B_{sc}\_C_8$. This trajectory can be mapped as the first initial condition check in the motion planning, where EW_1 has to be on $B_{sc}\_C_8$. Consider J_5's motion was tracked with J_1 fixed to $B_{sc}\_C_8$. Now, the second trajectory shows with EW_1's J_5 locked at $B_{sc}\_C_8$, J_1's motion is tracked to reach the mirror module in the storage spacecraft. The third trajectory shown has EW_1's J_5 fixed to $B_{sc}\_C_8$, J_1's motion is tracked to reach connector C_8 on the truss. This motion is a very common motion during mode:1 when EW_1 performs pick-and-place operation to fill in the left half outer-ring of the truss.

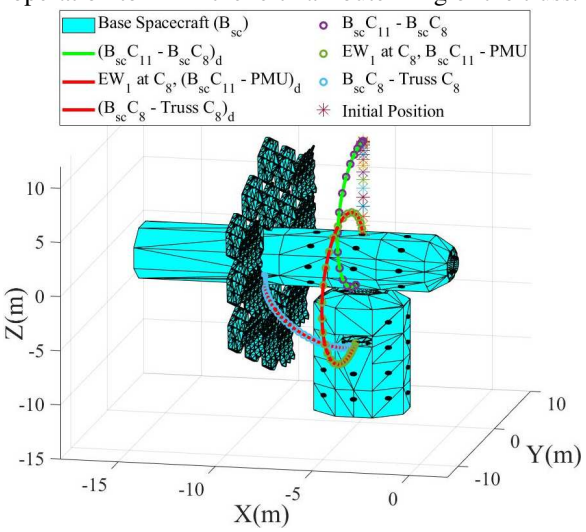

Figure 14. Simulated trajectory representing a real mission scenario

8 CONCLUSIONS

In this paper, a robotic in-orbit assembly of a 25 LAST is presented. An E-Walker is presented as the candidate architecture to assist with the assembly. The E-Walker's dynamic model and gait pattern are discussed. The E-Walker is controlled using a PID controller to track the desired joint trajectory within the joint torque limits. The key mission requirements were introduced and the features of LAST, base spacecraft and truss were stated. The strategies to implement a safe and smooth design is presented. A mission concept for the assembly of the 25m LAST using two E-Walkers is discussed elaborately with the help of an algorithm. Simulation results of the E-Walker following a straight-line trajectory for 3 cycles and a real-mission trajectory is shown with the E-Walker showcasing the desired performance.

9 FUTURE WORK

Future research involves analysing the performance of the system with non-linear control architectures, CAD modelling of the E-Walker along with Finite Element Analysis to assess the structural stability. The spacecraft dynamics would be incorporated and coupled with the E-Walker's dynamic model. A suitable grasping technology needs to be designed to facilitate a safe assembly of the 25m LAST. The autonomous assembly of the whole telescope including the secondary mirror, the booms, baffles etc. would be looked into with the help of the E-walker.

Acknowledgement

This research is funded by the University of Lincoln, UK. The authors would also like to express gratitude to Airbus for funding a precursor study that involved the Surrey Satellite Technology, Ltd. and the University of Surrey, UK.

References

[1] "NASA-SpaceX Dragon", *Nasa.gov*, 2020. [Online].
Available: https://www.nasa.gov/mission_pages/station/multimedia/gallery/iss034e062489.html.
[Accessed: 13- Sep- 2020].

[2] "Space versus Ground Telescopes", *UArizona Research, Innovation & Impact*, 2020. [Online]. Available: https://research.arizona.edu/stories/space-versus-ground-tele-scopes#:~:text=Compared%20to%20space%2Dbased%20telescopes,the%20cosmos%E2%80%94or%20space%20junk.
[Accessed: 13 Sep 2020]

[3] M. A. Roa, K. Nottensteiner, A. Wedler, G. Grunwald, Robotic Technologies for In-Space Assembly Operations, Proc. i-SAIRAS Conf., 2017

[4] M. Deremetz et al., "MOSAR: Modular Spacecraft Assembly and Reconfiguration Demonstrator", Proc. ASTRA 2019 symposium Noordwijk, Netherlands, 27-28 May 2019.

[5] M. Rognant et al., "Autonomous assembly of large structures in space: a technology review", Proc. 8th EUCASS, Madrid, Spain, 1-4 July 2019, DOI: 10.13009/EUCASS2019-685

[6] "UK Research and Development Roadmap", GOV.UK, 2020. [Online]. Available: https://www.gov.uk/government/publications/uk-research-and-development-roadmap/uk-research-and-development-roadmap. [Accessed: 13 Sep 2020]

[7] A. Nanjangud et al., "Towards robotic on-orbit assembly of large space telescopes: Mission architectures, concepts, and analysis", Proc. 70th IAC, Washington DC, USA, Oct 21-25, 2019.

[8] A. Nanjangud, P. C. Blacker, A. Young, C. M. Saaj, C. I. Underwood, S. Eckersley, M. Sweeting, and P. Bianco, "Robotic architectures for the on-orbit assembly of large space telescopes", Proc. ASTRA 2019 symposium, Noordwijk, Netherlands, 27-28 May 2019.

[9] S. Brooks, P. Godart, P. Backes, B. Chamberlain-Simon, R. Smith and S. Karumanchi, "An untethered mobile limb for modular in-space assembly", *2016 IEEE Aerospace Conference*, MT, USA, 2016.

[10] M. Spong, S. Hutchinson, and M. Vidyasagar, Robot Dynamics and Control, John Wiley & Sons, 2nd ed, 2005, ISBN – 0471649902

[11] J. Nelson, "Segmented mirror telescopes," in Optics in Astrophysics. Springer, 2006, pp. 61–72.

[12] A. A. Ata, "Optimal trajectory planning of manipulators: a review," Journal of Engineering Science and Technology, Vol. 2, No.1, pp. 32-54, April 2007

[13] A. Seddaoui and C. Saaj, \Combined Nonlinear H1 Controller for a Controlled Floating Space Robot", AIAA Journal of Guidance, Dynamics and Control, vol.42, no. 8, pp 1878-1885, 2019, doi: http://arc.aiaa.org/doi/abs/10.2514/1.G003811